



Santos, R. E.R.S., Silva, G. L.A., Santos, E. V., Duncan, S. M., Mottram, J. C. , Damasceno, J. D. and Tosi, L. R.O. (2017) A DiCre recombinase-based system for inducible expression in *Leishmania major*. *Molecular and Biochemical Parasitology*, 216, pp. 45-48.
(doi:[10.1016/j.molbiopara.2017.06.006](https://doi.org/10.1016/j.molbiopara.2017.06.006))

This is the author's final accepted version.

There may be differences between this version and the published version. You are advised to consult the publisher's version if you wish to cite from it.

<http://eprints.gla.ac.uk/143314/>

Deposited on: 05 July 2017

Enlighten – Research publications by members of the University of Glasgow
<http://eprints.gla.ac.uk>

A DiCre recombinase-based system for inducible expression in *Leishmania major*

Renato E. R. S. Santos¹, Gabriel L. A. Silva¹, Elaine V. Santos¹, Samuel M. Duncan², Jeremy C. Mottram^{2,3}, Jeziel D. Damasceno^{1*} and Luiz R. O. Tosi^{1*}

¹Department of Cell and Molecular Biology; Ribeirão Preto Medical School, University of São Paulo; Ribeirão Preto, SP, Brazil.

² Wellcome Centre for Molecular Parasitology, Institute of Infection, Immunity and Inflammation, University of Glasgow, United Kingdom.

³Centre for Immunology and Infection, Department of Biology; University of York; York, UK.

* To whom correspondence should be addressed. jezielbqi@gmail.com and luiztosi@fmrp.usp.br Tel: + 55 16 36023117; Fax: +55 16 36020728.

Highlights

- A DiCre recombinase-based system for inducible expression in *Leishmania major* is presented.
- The system is dose and time dependent
- The system mediates the expression of target genes from both integrated and episomal contexts

Abstract

Here we present the establishment of an inducible system based on the dimerizable Cre recombinase (DiCre) for controlled gene expression in the protozoan parasite *Leishmania*. Rapamycin-induced DiCre activation promoted efficient flipping and expression of gene products in a time and dose-dependent manner. The DiCre flipping activity induced the expression of target genes from both integrated and episomal contexts broadening the applicability of the system. We validated the system by inducing the expression of both full length and truncated forms of the checkpoint protein Rad9, which revealed that the highly divergent C-terminal domain of Rad9 is necessary for proper subcellular localization. Thus, by establishing the DiCre-based inducible system we have created and validated a robust new tool for assessing gene function in *Leishmania*.

Keywords: DiCre recombinase; *Leishmania*; inducible expression; DNA damage response; 9-1-1 complex; Rad9-Rad1-Hus1.

The genus *Leishmania* encompasses over 20 species, including those that are the causative agents of devastating human diseases worldwide collectively called leishmaniasis [1]. The *Leishmania* genome is organized in directional gene clusters that may include hundreds of genes from which transcription occurs in a polycistronic fashion. No canonical RNA Pol II promoters have been identified in this parasite and gene expression regulation seems to have been devolved to post-transcriptional processes [2]. The remarkable genome plasticity of *Leishmania*, which leads to frequent genome rearrangements, not only impacts gene expression control, but also hinders the genetic manipulation of the parasite [3,4]. Therefore, a dependable and robust genetic toolkit is necessary for effective post-genomic functional studies in this protozoan.

Over the past decades, a collection of genetic manipulation tools for *Leishmania* has been introduced. For instance, transient and stable transfection, gene replacement and disruption, expression vectors and functional complementation and rescue are well-established and reliable tools [5–7]. More recently, the introduction of protein stabilization strategies [8,9] a tetracycline-inducible system for protein expression [10], the dimerizable Cre recombinase (DiCre)-based system for inducible knockouts [11,12] and the establishment of CRISPR cas9 genome editing [13] has further improved our capacity to address peculiar aspects of this parasite's biology. Given the stringent regulation of DiCre recombinase activity and the variety of strategies for genetic regulation conferred by the use of loxP recombination sites [14,15], we decided to adapt the DiCre-based inducible system for controlled gene expression in *Leishmania major*. Our strategy involves the generation of a cell line constitutively expressing DiCre recombinase and carrying an inverted gene of interest flanked by *cis* orientated loxP sites. These constructs are integrated into the 18S rRNA locus and expressed under the control of the Pol I promoter. The antisense orientation of the gene of interest prevents transcription of coding RNA from the positive strand until activation of DiCre recombinase activity by rapamycin treatment. Once activated, DiCre catalyzes the 'flip' of the sequence flanked by *cis* loxP sites, resulting in transcription of a coding RNA and subsequent protein expression (Figure S1A). To prevent continual gene 'flipping' by loxP site recombination we employed left-element mutant (lox66) and right-element mutant (lox77) sites [16]. These mutated lox sequences act as sites of recombination to generate a wild-type loxP site and a double mutant Lox72 site for which DiCre has a dramatically reduced affinity. As such, a single recombination event is favoured upon DiCre recombinase induction, thereby preventing re-inversion, leading to continual expression of the gene of interest (Figure S1B).

The advantages of this approach include: (i) the use of fewer transfection rounds and, consequently, fewer selectable markers when compared to the tetracycline-inducible system developed for *L. mexicana* by Kraeva and colleagues [10]; (ii) the possibility to induce expression of gene products from both chromosomal and/or episomal contexts; (iii) the system promotes a non-leaky expression that can be induced in a time and dosage-dependent manner; (iv) the possibility to compare the expression of endogenous and mutated proteins including the conditional expression of deleterious gene products.

To create the system, plasmid pGL2339 (Figure S2A) was digested and the array encoding the blasticidin resistance cassette and the dimerizable Cre recombinase subunits was integrated into the ribosomal locus to generate the DiCre^{SSU} cell line (Figures 1A and Table S2). Next, the plasmid pGL2332 (Figure S2B) was digested and the lox66/lox77-flanked 6xHA-GFP cassette containing the puromycin resistance marker was integrated into the ribosomal locus of the DiCre^{SSU} cell line to generate the GFP^{fllox} cell line (Figures 1B and Table S2). Both integration events were confirmed by PCR analysis, which also ascertained that the 6xHA-GFP coding sequence was present in the antisense orientation in the GFP^{fllox} cell line (Figure 1C). To test the system and the DiCre flipping activity, the GFP^{fllox} cell line was incubated with the DiCre dimerization ligand, rapamycin, and the inversion of the GFP cassette was confirmed by PCR analysis using the appropriate set of primers (Figure 1D). Semi-quantitative PCR analysis showed that the flipping reaction is time dependent and seem to reach its maximal level around 96 hours after induction (Figure S3). Importantly, flipping of the GFP cassette in the absence of rapamycin was not detectable in the PCR analyses shown in Figure 1D or Figure S3, indicating a non-leaky DiCre activity in the GFP^{fllox} cells. Upon rapamycin induction, expression of 6xHA-GFP was detectable after 12 hours and its levels were dose and time-dependent (Figure 1E). Consistently, 6xHA-GFP was not detectable in the absence of rapamycin, further confirming the stringent regulation of the system (Figure 1E). We further used immunofluorescence analysis (IFA) to examine the expression profile within the population and observed that 6xHA-GFP was detectable by IFA only after rapamycin incubation (Figure 1F). Consistent with the western blot analysis, the IFA also demonstrated the rapamycin dose-dependence of the system (Figure S3) further confirmed by the quantification of GFP corresponding signal (Figure 1G). Besides confirming the tight regulation of the system, this set of data also demonstrates that the system is suitable for subcellular compartmentalization studies in this parasite.

To expand the limits of the system we tested it for the ability to flip sequences from an episome, which can be found in multiple copies in the cell. To that end, the plasmid pGL2332 was transfected into the DiCre^{SSU} cell line to generate the pGFP^{flox} cell line (Figure 1H). PCR analysis confirmed the DiCre background and the presence of the target plasmid (Figure 1I), and the flipping of the 6xHA-GFP cassette upon rapamycin incubation (Figure 1J). Consistently, western blot analysis confirmed the expression of the cassette exclusively in rapamycin treated cells (Figure 1K). These results further demonstrate the tight control of DiCre activity and greatly extend the applicability of the system as a reliable tool for inducible protein expression not only from the genomic context, but also from episomal targets. It is noteworthy that this system it is not expected to be reversible, which can be a disadvantage if reversion of the expressed phenotype is required. However, the irreversibility of the system can be taken an advantageous feature to be explored in both *in vitro* and *in vivo* infections assays where inclusion of selection drugs and rapamycin might not be desired.

To further validate the DiCre flipping tool we used the protein Rad9, which participates in the *Leishmania* DNA Damage Response as part of the checkpoint clamp 9-1-1 [17,18]. In eukaryotic cells, Rad9 has an unstructured C-terminal domain that corresponds to ~1/3 of the protein and is necessary for its function in signalling genotoxic stress [19]. The unstructured C-domain of *Leishmania* Rad9 is ~3.5x longer than its human counterpart (Figure 2A) and, so far, no function has been reported for this C-terminal extension. To start exploring the function of this C-terminal domain, Rad9 full length or C-terminal truncated encoding sequences, were cloned into the pGL6000 vector (Figure S2C), to generate the Rad9-6xHA^{flox} and Rad9 Δ C'-6xHA^{flox} cassettes, respectively. These constructs were digested and integrated into the ribosomal locus of the DiCre^{SSU} cell line to generate the Rad9^{flox} and Rad9 Δ C'^{flox} cell lines, respectively (Figure 2B and Table S2). Proper Integration was confirmed by PCR analysis (Figure 2C) and, as expected, flipping of the cassettes was detected exclusively upon rapamycin incubation (Figure 2D). Accordingly, expression of Rad9-6xHA and Rad9 Δ C'-6xHA was detectable at comparable levels after induction with rapamycin, as demonstrated by western blot analysis (Figure 2E; upper panel). Anti-Rad9 polyclonal serum was used in western blot analysis to evaluate changes in total Rad9 levels (i.e. Rad9-6xHA plus endogenous Rad9) in the Rad9^{flox} cell line after DiCre activation (Figure 2E; middle panel). Our analysis indicated that, upon induction, Rad9-6xHA was overexpressed when compared to the endogenous Rad9. Quantification of Rad9 signal revealed that

up to ~65% of the total Rad9 expressed in these cells corresponded to the induced version of the protein demonstrating that the system can mediate overexpression. Interestingly, the induction of Rad9-6xHA resulted in significant decrease in the levels of endogenous Rad9. However, the same effect was less pronounced when the truncated Rad9 Δ C'-6xHA was expressed (Figure 2E; middle panel and Figure 2F). These data suggest that *Leishmania* Rad9 levels are under tight regulation, which probably involves the participation of its C-terminal extension. Whether this requires a direct or indirect role of this domain remains to be investigated. We were not able to properly assess Rad9 Δ C'-6xHA levels relative to endogenous Rad9 using the polyclonal anti-Rad9 serum. One reason for this is that anti-Rad9 serum detects a faster migrating protein with the same molecular mass as Rad9 Δ C'-6xHA, hindering its detection. Similarly to the endogenous Rad9, the level of this protein was also reduced upon induction of Rad9-6xHA (Figure 2E; middle panel). While the presence of this band could represent cross-detection of an unrelated protein, these data suggest that it could be a processed form of Rad9 and further characterization is needed to clarify this.

We also analysed the effect of the deletion of the C-terminal extension on the Rad9 subcellular localization. Using IFA, we observed that in the majority of the cells Rad9-6xHA was almost exclusively found in the nuclear compartment, as previously described for Rad9 [17] (Figures 2G and S4). On the other hand, truncated Rad9 Δ C'-6xHA presented a less defined localization being prominently detected in the cytoplasm of the majority of the cells (Figure 2G and S4). Consistently, quantitative analysis of the IFA data showed that Rad9-6xHA signal is concentrated in the region containing the nuclear DNA staining, while Rad9 Δ C'-6xHA signal expands beyond the nuclear staining limits (Figure 2H). Based on these data, it is reasonable to conclude that the C-terminal extension is necessary for proper subcellular distribution of Rad9 in *Leishmania*.

In summary, we have demonstrated that the DiCre-based expression system described here is a valuable addition to the *Leishmania* genetic manipulation toolkit. Its use to study the parasite Rad9 revealed important features of the protein, produced reagents for future studies and proved its value for functional analyses in this parasite.

Acknowledgments

This work was supported by FAPESP - Fundação de Amparo à Pesquisa no Estado de São Paulo grants 14/06824-8, 14/00751-9, 13/00570-1 and 13/26806-1,

the Medical Research Council (MR/K019384) and the Wellcome Trust [104111]. The Confocal Microscopy Laboratory was supported by FAPESP 04/08868-0. The Multiphoton Microscopy Laboratory was supported by FAPESP 09/54014-7. Roberta Ribeiro Costa Rosales and Elizabete Rosa Milani for assistance with microscopy experiments.

Author contribution

RERSS performed the experiments, collected data, and critically revised the manuscript. GLAS generated and analysed the pGFP^{flox} cell line. EVS conducted the anti-Rad9 western blot analysis in Figure 2E. SMD and JCM generated pGL2332 and pGL2339 plasmids, provided reagents and critically revised the manuscript. JDD generated the DiCre^{SSU} cell line, planned experiments, performed analysis presented in Figure 2A, helped acquire data of Figure 2G and wrote the manuscript. LROT planned experiments and wrote the manuscript.

References

- [1] J. Alvar, I.D. Vélez, C. Bern, M. Herrero, P. Desjeux, J. Cano, J. Jannin, M. den Boer, the W.L.C. Team, Leishmaniasis Worldwide and Global Estimates of Its Incidence, *PLoS One*. 7 (2012) e35671.
- [2] S. Martínez-Calvillo, S. Yan, D. Nguyen, M. Fox, K. Stuart, P.J. Myler, Transcription of *Leishmania major* Friedlin Chromosome 1 Initiates in Both Directions within a Single Region, *Mol. Cell*. 11 (2003) 1291–1299.
- [3] J.-M. Ubeda, D. Légaré, F. Raymond, A. Ouameur, S. Boisvert, P. Rigault, J. Corbeil, M.J. Tremblay, M. Olivier, B. Papadopoulos, M. Ouellette, Modulation of gene expression in drug resistant *Leishmania* is associated with gene amplification, gene deletion and chromosome aneuploidy, *Genome Biol*. 9 (2008) R115.
- [4] M.B. Rogers, J.D. Hilley, N.J. Dickens, J. Wilkes, P.A. Bates, D.P. Depledge, D. Harris, Y. Her, P. Herzyk, H. Imamura, T.D. Otto, M. Sanders, K. Seeger, J.-C. Dujardin, M. Berriman, D.F. Smith, C. Hertz-Fowler, J.C. Mottram, Chromosome and gene copy number variation allow major structural change between species and strains of *Leishmania*., *Genome Res*. 21 (2011) 2129–42.
- [5] J.H. LeBowitz, C.M. Coburn, S.M. Beverley, Simultaneous transient expression assays of the trypanosomatid parasite *Leishmania* using β -galactosidase and β -glucuronidase as reporter enzymes, *Gene*. 103 (1991) 119–123.
- [6] J.D. Damasceno, S.M. Beverley, L.R.O. Tosi, A transposon toolkit for gene transfer and mutagenesis in protozoan parasites., *Genetica*. 138 (2010) 301–11.
- [7] S.M. Duncan, N.G. Jones, J.C. Mottram, Recent advances in reverse genetics of *Leishmania*: manipulating a manipulative parasite., Unpubl. Data. (2017).
- [8] L. Madeira da Silva, K.L. Owens, S.M.F. Murta, S.M. Beverley, Regulated expression of the *Leishmania major* surface virulence factor lipophosphoglycan using conditionally destabilized fusion proteins, *PNAS*. 106 (2009) 7583–8.
- [9] L. Podešvová, H. Huang, V. Yurchenko, Inducible protein stabilization system in *Leishmania mexicana*, *Mol. Biochem. Parasitol*. 214 (2017) 62–64.
- [10] N. Kraeva, A. Ishemgulova, J. Lukeš, V. Yurchenko, Tetracycline-inducible gene expression system in *Leishmania mexicana*, *Mol. Biochem. Parasitol*. 198 (2014) 11–13.
- [11] S.M. Duncan, E. Myburgh, C. Philippon, E. Brown, M. Meissner, J. Brewer, J.C. Mottram, Conditional gene deletion with DiCre demonstrates an essential role for CRK3 in *Leishmania mexicana* cell cycle regulation, *Mol. Microbiol*. 100 (2016) 931–944.
- [12] T. Beneke, R. Madden, L. Makin, J. Valli, J. Sunter, E. Gluenz, A CRISPR Cas9 high-throughput genome editing toolkit for kinetoplastids, *R. Soc. Open Sci*. 4 (2017) 170095.
- [13] F.A. Ran, P.D. Hsu, J. Wright, V. Agarwala, D.A. Scott, F. Zhang, Genome engineering using the CRISPR-Cas9 system, *Nat. Protoc*. 8 (2013) 2281–2308.
- [14] G.D. Van Duynes, A Structural View of Cre- *loxP* Site-Specific Recombination, *Annu. Rev. Biophys. Biomol. Struct*. 30 (2001) 87–104.
- [15] N. Jullien, F. Sampieri, A. Enjalbert, J.-P. Herman, Regulation of Cre recombinase by ligand-induced complementation of inactive fragments., *Nucleic Acids Res*. 31 (2003) e131.
- [16] H. Albert, E.C. Dale, E. Lee, D.W. Ow, Site-specific integration of DNA into wild-type and mutant *lox* sites placed in the plant genome., *Plant J*. 7 (1995) 649–59.
- [17] J.D. Damasceno, V.S. Nunes, L.R.O. Tosi, LmHus1 is required for the DNA

- damage response in *Leishmania major* and forms a complex with an unusual Rad9 homologue, *Mol. Microbiol.* 90 (2013) 1074–1087.
- [18] J.D. Damasceno, R. Obonaga, E. V. Santos, A. Scott, R. McCulloch, L.R.O. Tosi, Functional compartmentalization of Rad9 and Hus1 reveals diverse assembly of the 9-1-1 complex components during the DNA damage response in *Leishmania*, *Mol. Microbiol.* 101 (2016) 1054–1068.
- [19] V.M. Navadgi-Patil, P.M. Burgers, The unstructured C-terminal tail of the 9-1-1 clamp subunit Ddc1 activates Mec1/ATR via two distinct mechanisms., *Mol. Cell.* 36 (2009) 743–53.

Legends to Figures

Figure 1. Establishment of an inducible DiCre-based expression system in *L. major*. **(A)** Schematic representation (not in scale) of the cassette encoding the truncated forms of DiCre after integration into the 18S ribosomal RNA locus (SSU) of *L. major* wild type cell (LT252) to generate the DiCre^{SSU} cell line; BLA: blasticidin resistance marker. **(B)** Schematic representation (not in scale) of the 6xHA-GFP cassette (see Figure S1B for details) after integration into the SSU locus of the DiCre^{SSU} cell line (A) to generate the GFP^{flox} cell line; PAC: puromycin resistance marker; upon rapamycin (RAP) addition, the indicated lox sites mediate the flipping of 6xHA-GFP cassette allowing its expression. In (A) and (B), black arrows indicate approximate annealing position of primers used for PCR analysis. **(C)** PCR analysis of genomic DNA (gDNA) using the indicated set of primers (annealing positions shown in (A) and (B)); DHFR-TS was the loading control for all PCR analyses presented in this work. **(D)** PCR analysis of gDNA from GFP^{flox} cells cultivated in the presence (+) or absence (-) of 100nM RAP for 48h; primers are indicated below each panel (see annealing positions in (B)). **(E)** Western blot analysis of total cell extracts from the GFP^{flox} cells cultivated with RAP for the indicated periods of time; two distinct cell-equivalent amount of extracts was analysed; anti-HA was used to detect 6xHA-GFP; EF1 α was the loading control. **(F)** Immunofluorescence analysis of GFP^{flox} cells cultivated in the presence (+) or absence (-) of 100nM RAP for 48h; images were acquired with a DMI 6000B inverted microscope (Leica); n and k indicate nuclear and kinetoplast DNA, respectively; scale bar = 5 μ m. **(G)** GFP^{flox} cells were subject to immunofluorescence as in (F) after cultivation with RAP for 48h; signal corresponding to 6xHA-GFP from individual cells was quantified using Image J software; bars indicate mean +/- Standard Deviation (S.D.); p values by Kruskal-Wallis test were: (**)= 0.0057; (***) = 0.0008. **(H)** The plasmid pGL2332 (Figure S1B) was transfected as a circular episome in the DiCre^{SSU} cells to generate the pGFP^{flox} cell line; as in (B), RAP addition is expected to induce expression of 6xHA-GFP; schematic representations are not in scale. **(I)** PCR analysis of gDNA using the indicated set of primers (annealing positions shown in (A) and (H)). **(J)** PCR analysis of gDNA from pGFP^{flox} cells cultivated in the presence (+) or absence (-) of 100nM RAP for 48h; primers are indicated below each panel (see annealing position in (H)). **(K)** Western blot analysis of total cell extracts from the pGFP^{flox} cells cultivated in the presence (+) or absence (-) of 100nM RAP for 48h; anti-HA was used to detect 6xHA-GFP; EF1 α was the loading control.

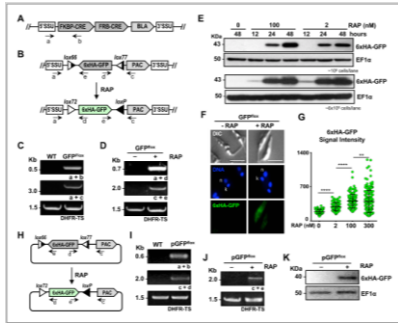


Figure 2. Expression of Rad9 and Rad9 Δ C' using the DiCre-based inducible system. (A) Predicted amino acid sequence of Rad9 from *L. major* (LmjF.15.0980) and *Homo sapiens* (NP_004575.1) were subject to disorder prediction using IUPred (<http://iupred.enzim.hu>); values above 0.5 (horizontal black dotted line) can be considered as disordered regions; horizontal grey bars above each graph indicate the Rad9 domain (Pfam: PF04139) and the disordered C-terminal domain; C-terminal domain of human Rad9 and the corresponding region in *L. major* Rad9 is indicated as C; the extended C-terminal of *L. major* Rad9 is indicated as C'. **(B)** Full length Rad9 from *L. major* or a truncated version lacking the C-terminal extension (C'), were cloned as C-terminal fusion with a 6xHA tag to generated the Rad9-6xHA^{flox} and Rad9 Δ C'-6xHA^{flox} constructs (not in scale); Rad9-6xHA and Rad9 Δ C'-6xHA constructs are arranged in an inverted orientation, flanked by the indicated lox sequences and were integrated into the ribosomal locus (SSU) of the DiCre^{SSU} cells (see Figure 1A) to generate the Rad9^{flox} and Rad9 Δ C'^{flox} cell lines, respectively; black arrows indicate approximate annealing position of oligonucleotides used for PCR analyses; PAC: puromycin resistance marker. **(C)** PCR analysis of gDNA using the indicated set of primers (see annealing positions in (B)). **(D)** PCR analysis of gDNA from cells cultivated in the presence (+) or absence (-) of 100nM RAP for 48h; primers are indicated below each panel (see annealing positions in (B)). **(E)** Western blot analysis of total cell extracts from the indicated cells cultivated in the presence (+) or absence (-) of RAP for 48 hours; anti-HA (upper panel) and anti-Rad9 (bottom panel) was used to detect Rad9-6xHA Rad9 Δ C'-6xHA; a protein with a similar migration pattern of Rad9 Δ C'-6xHA is detected by anti-Rad9 and is indicated with (*); GAPDH was the loading control. **(F)** Levels of endogenous Rad9 in western blot analysis shown in (E) were determined and normalized with the GAPDH signal, using Image J software; signal from cells exposed to RAP was plotted as a fraction relative to signal from respective non-induced culture. **(G)** Immunofluorescence analysis of the indicated cells cultivated in the presence (+) or absence (-) of 100nM RAP for 48h; images are representative of a Z-maximal projection from 14 Z-slices acquired with a multiphoton system coupled with LMS780 AxioObserver microscope (Zeiss); n and k indicate nuclear and kinetoplast DNA, respectively; black bars on the DIC field indicate the section where quantification shown in (H) was performed; n and k indicate nuclear and kinetoplast DNA, respectively; scale bar (white) = 5 μ m. **(H)** Signal corresponding to DAPI, Rad9-6xHA and Rad9 Δ C'-6xHA in the section indicated by the black bar in (G) was quantified with ImageJ.

